

Induced defect levels of P and Al vacancy-complexes in 4H-SiC: A hybrid functional study

E. Igumbor^{a,b,*}, O. Olaniyan^a, R. E. Mapasha^a, H. T. Danga^a, E. Omotoso^a, W. E. Meyer^{a,**}

^a*Department of Physics, University of Pretoria, Pretoria 0002, South Africa*

^b*School of Interdisciplinary Research and Graduate Studies, University of South Africa, UNISA 0003, Preller Street, Pretoria, South Africa*

Abstract

The electronic behaviour of high-dose phosphorus implanted in 4H-SiC is mainly desirable to obtain lower sheet resistance of 4H-SiC. Al doping on the other hand acts as an acceptor, improves the dielectric properties of 4H-SiC and has very low diffusivity in SiC. Using a hybrid density functional theory, we investigated the properties of Al and P defect-complexes in 4H-SiC a wide band-gap semiconductor that is promising for applications in high-frequency and high-temperature electronic device. We show that vacancy-complexes formed by P_{Si} and Al_{Si} are more energetically stable than those formed by P_C and Al_C. The defects with silicon vacancy are predicted to experience more lattice distortion compared to those formed with carbon vacancy. While vacancy-complexes formed with P_{Si} or P_C and V_C induced double donor levels, vacancy-complex formed with substitution of P and V_{Si} induced negative-U charge state ordering. The Al with V_C related vacancy-

*Corresponding author

**Corresponding author

Email addresses: elgumuk@gmail.com (E. Igumbor), wmeyer@up.ac.za (W. E. Meyer)

complexes induced deep single donor and acceptor levels, and Al with V_{Si} induced only acceptor and negative-U ordering.

Keywords: Defect, formation energy, charge state, complexes

1. Introduction

One of the most promising wide band gap semiconductors is SiC. This is owing to the fact that its well known polytypes ($2C$, $3C$, $4H$, $6H$) have significant application in extremely severe harsh environments (high-temperature, high-frequency, and high-power electronic devices). The $4H$ -SiC amongst the commercially available SiC polytypes is more promising for application in metal-oxide-semiconductor field-effect-transistors (MOSFETs) high-power electronic devices . This is as a result of $4H$ -SiC having a relatively high bulk electron mobility and small anisotropy compared to other well known polytypes [1]. The application of $4H$ -SiC for high-power electronic device is not free from defects activities. Defects are known to influence the performance of wide or narrow band gap semiconductor materials including $4H$ -SiC. Defects that enhances the performance of a device are desirable and should intentionally introduced [2, 3, 4]. Several experimental [5, 6, 7, 8, 9, 10, 11, 12, 13, 14, 15, 16, 17] and theoretical [18, 19, 20, 21, 22] (most especially using the well known density functional theory) studies of point defects in $4H$ -SiC have been reported. Point defects such as substitution, interstitials, vacancy and defect-complexes (interstitial-complex, vacancy-complex or antisite) have been reported in literature [18, 19, 23, 24, 25, 26]. Report on the nuclear transmutation proceeding under high energy doping of Si and SiC by P suggests that an n -type phosphorus doped layer induced radiation

damage defects in SiC [27]. To realized a high-performance SiC electronic device, electronic behaviour of high-dose phosphorus-ion implanted $4H$ -SiC was reported by Negoro *et al.* [28]. This researcher suggests that in order to reduce the resistivity of Ohmic contacts as well as source and drain regions in field-effect transistors (FET), ion implantation with a high donor dose into SiC is required. As a result, N or P implantation is commonly used for this purpose. P implantation has been used to obtained lower sheet resistance in $4H$ -SiC [29]. Recently, Okamoto *et al.* [30] have shown that an improved channel mobility of $4H$ -SiC MOSFETs on Si face through P doped gate oxide is attainable. SiC is the only known wide band gap material that grows a thermal oxide (SiO_2), which makes it well suitable for the fabrication of MOSFETs [31]. This possibility comes with some challenges of deteriorating high density of interface at $\text{SiO}_2/4H$ -SiC. However, studies have shown that the interface state density can be decreased by over oxidation of P implanted in $4H$ -SiC substrates [1, 30, 32]. Phosphorus implanted into $6H$ -SiC shows ionization energies of 80 and 110 meV for the hexagonal and cubic lattice sites, respectively. These ionization energies are almost equivalent to those observed for nitrogen [17]. Whereas as reported in Ref. [33], where low sheet resistance is required in a device, it is advantageous to replace N with P. This is based on the fact that with comparable doping, thermal processing under equilibrium conditions, sheet resistances of P-implanted in $4H$ -SiC are in an order of magnitude lower than those measured in N-implanted in $4H$ -SiC [34]. While the ionisation energies of P implanted in $4H$ -SiC is about 0.10 eV higher than those of N-implanted, the carrier concentration of the former is about a factor of five lower than the latter when subjected under

annealed temperature of 3000 °C. Although not with the expense of higher mobility for the P-implanted in 4H-SiC which does not offset the lower concentration and making the resistivity of P-implanted in 4H-SiC to be higher than those of the N-implanted in 4H-SiC. While for low dose application, one will consider the N-implanted to be energetically favourable, but on the contrary for high dose application and sheet reduction, P implanted in 4H-SiC is desired [35]. During the implantation of P in 4H-SiC, it is expected to caused crystal damage and introduced new defects which could enhance the performance or on the worse case scenario, act as a recombination centre therefore decreasing the operational power of the device. Despite the fact that small scale production of SiC power FET and Schottky barrier have started, there are varieties of point and extended defects still present in SiC epitaxial wafers [36]. Bockstedte *et al.* [37] have previously reported abundance of P and N related defects using an ab initio method. The researchers shown that the calculation of formation energies give access to the electrically active defects. According to Ref. [37] complexes with vacancy, antisite and interstitial are suggested to be stable. Furthermore, Bockstedte *et al.* [37] suggests that the phosphorus-vacancy complexes activation is only limited by the onset of precipitation. Al, a *p*-type dopant in 4H-SiC has a low diffusivity and a high solubility [38]. But a well know basic physical problem is the low ionisation rate of *p*-type impurity atoms. For example, experimental results on donor-acceptor pair luminescence show that the ionisation of Al_{Si} lies within the value of 0.20-0.19 eV [39]. Al is mainly introduced in 4H-SiC via ion implantation. Al related defect-complexes in 4H-SiC has been reported, where it was established that aluminium can form thermally stable

complexes with carbon interstitial (C_i) and carbon vacancy (V_C) inducing deep levels in the band gap [40, 41]. Al defect-complex is suggested as a possible reason for the imperfect activation rate of a shallow aluminium acceptor in the damaged region of Al-implanted in SiC. Despite the fact that several studies on defects in $4H$ -SiC have been theoretically [37, 40, 41] reported (for interstitial, vacancy, substitution, interstitial-complexes, vacancy-complexes or antisites), there are more that need to be investigated either experimentally or theoretically. For example complexes formed with N and either C or Si vacancy or interstitial have been reported, but detail reports on P or Al complexes formed with either V_C or V_{Si} are lacking and hence the motivation of this study.

In this report, we have used the Heyd, Scuseria and Ernzerhof (HSE06) [42] hybrid functional within the framework of the density functional theory (DFT) to model the electronic and total energies of P or Al related vacancy-complexes in $4H$ -SiC. The formation energy and binding energies as well as the thermodynamic charge state transition energies were calculated. While our results reveal that the vacancy-complexes with a carbon vacancy induced both donor and acceptor levels, the vacancy-complexes with silicon vacancy exhibit the properties of negative-U ordering in the band gap of $4H$ -SiC. The complexes with a silicon vacancy experienced more lattice distortion compared to those formed with a carbon vacancy.

2. Computational details

DFT based on the generalized Kohn-Sham theory method as implemented within the Vienna *Ab-initio* Simulation Package (VASP) [43, 44] was used

to perform all first principle calculations. the projector-augmented wave (PAW) method [43, 45] was used to describe the valence electrons, and the exchange-correlation functional was approximated using the HSE06 hybrid functional with generalized gradient approximation (GGA) functional of Perdew, Burke, and Ernzerhof (PBE) [46]. The HSE06 functional provides partial cancellation of self-interaction and has been used to predict accurate structural, energetics and band structures of semiconductor materials [47, 48]. This is in contrast to the local density approximation (LDA) or the GGA which severely underestimate band gap of materials and thereby wrongly predicting the electrically active induced defect levels in the band gap [20, 49, 50, 51]. For the HSE06, a default mixing parameter of 25% and 0.2 \AA^{-1} screening parameter was used for all calculations. It is sufficient to say that the 25% fraction of exact Hartree-Fock exchange and 0.2 \AA^{-1} screening parameter were enough to predict a band gap of 3.23 eV (see Fig. 1) for the $4H$ -SiC, which is in agreement with the experimental value of 3.26 eV at 300 K [52]. The $4H$ -SiC has a hexagonal cubic structure with the space group P_6-3mc for its unit cell. The optimized lattice constants and band gap for the $4H$ -SiC unit cell were obtained using a Monkhorst-Pack [53] grid of $8 \times 8 \times 8$. A kinetic energy cutoff of 400 eV was used for the expansion of one-electron Kohn-Sham wave functions on the plane-wave basis. Furthermore, the cell was relaxed until the minimum total energy difference was less than 10^{-5} eV. Equilibrium configurations of all the atomic geometries were allowed to relax freely until the Hellmann-Feynman forces acting on each atom was less than 0.01 eV/\AA . The calculated lattice parameters $a = 3.07 \text{ \AA}$, $c = 10.05 \text{ \AA}$ and $c/a = 3.27$, are in good agreement with experimental values

of 3.07 Å, 10.05 Å and 3.27 [52, 54], respectively. Defect calculations are suitably performed using periodic supercell with boundary conditions. For the defect calculation, a $2 \times 2 \times 2$ supercell of 96 atoms containing 48 each of Si and C atom was created from the repeated optimized unit cell. The supercell atomic positions were relaxed using the same convergence criteria as of the unit cell but with a reduced $2 \times 2 \times 2$ Monkhorst-Pack k-point grid. More information about the convergence criteria of the supercell can be found in our previous report [26]. Inside the supercell, a P atom was substituted at either C or S atomic site and a C or Si vacancy was created to form a P related vacancy-complex. This same procedure was repeated for the Al related vacancy-complexes. This is followed by atomic relaxation with the same conditions as the pristine 96 atoms supercell of the $4H$ -SiC. Spin polarization was included in all calculations involving V_{Si} , this is to account for the spin dependency of V_{Si} [55, 56, 57]. A vacancy-complex formation energy $E^F(vacancy - complex, q)$ as a function of electron Fermi energy (ε_F) is given as [58, 59]

$$\begin{aligned}
E^F(vacancy - complex, q) = & E(vacancy - complex, q) - E(4H - SiC) \\
& + \sum_i \Delta(n)_i \mu_i + q[E_{VBM} + \varepsilon_F] + E_{FNV}^q,
\end{aligned} \tag{1}$$

where the total energy of the vacancy-complex, total energy of the pristine supercell of $4H$ -SiC, number of removed or added constituent atoms of type i th and the energy of the valence band maximum (VBM) are represented by $E(vacancy-complex, q)$, $E(4H - SiC)$, $\Delta(n)_i$ and E_{VBM} , respectively. When modelling defect using the periodic boundary condition supercell approach,

the problems of spurious interaction of charged defects and finite-size effects on the total energies arise. These arising errors were properly corrected by including E_{FNV}^q in Eq. 1 according to the method proposed by Ref [60]. The μ_i in Eq. 1 is the chemical potential of the type *ith* constituent atom. The chemical potentials μ_{Si} for Si, μ_C for C, μ_P for P and μ_{Al} for Al should satisfy the stability condition for bulk SiC. The $\Delta\mu$, the effective chemical potential of the constituent of the compound must satisfy the condition $\|\Delta\mu\| \leq \Delta H_f$, where ΔH_f (0.62 eV from our calculation [26]) is the heat of formation. In a perfect stoichiometry growth, $\Delta\mu$ must be equal to zero. In practice, stoichiometry of SiC is usually influence by the ratio of C and Si with the precursors C_3H_3 and SiH_4 , respectively. When $\Delta\mu = \Delta H_f$, it shows that the crystal is under Si-rich condition whereas when the $\Delta\mu = -\Delta H_f$, the crystal is under C-rich conditions. Furthermore, under extremely Si-rich conditions the $\Delta\mu = \Delta H_f/2$ whereas for $\Delta\mu = -\Delta H_f/2$ indicates extremely C-rich conditions. In this report, the bulk μ_{Si} and μ_C were respectively calculated using the bulk silicon and diamond structure. While the μ_P was calculated using the converged energy of P body centered cube (BCC) structure, the μ_{Al} was calculated using the Al face centered cube structure (as the total energy per number of Al atom). Our calculation which is in agreement with literature [61, 62, 63] shown that under equilibrium conditions, the V_C and V_{Si} are energetically favourable with respect to their formation energies under Si-rich and C-rich conditions, respectively. As a result, the formation energies of the vacancy-complexes formed with V_C and V_{Si} were obtained under Si-rich and C-rich conditions, respectively, which is also in agreement with literature [64, 65]).

One of the interesting properties of defect in semiconductor is the electrical levels induced in the band gap of the material. The electrically induced defect levels in a band gap of a semiconductor can be ascertained theoretically by calculating the thermodynamic charge states transition level. The charge states transition level is the Fermi level where two different charge states (q and q') of the same defect have the same formation energy. This is calculated using Eq. 2.

$$\epsilon(q/q') = \frac{E(Q) - E(Q')}{q' - q}, \quad (2)$$

where $E(Q) = E^F(\text{vacancy-complex}, q; \varepsilon_F = 0)$ and $E(Q') = E^F(\text{vacancy-complex}, q'; \varepsilon_F = 0)$. According to Eq. 2, a charge state is thermodynamically stable and accessible when the Fermi level is below this energy: otherwise the charge state is not stable. Defect-complexes are found to be either stable or unstable (dissociates into non-interacting defects) depending on their binding energies. The binding energy E_b which is the energy required to split up a vacancy-complex into well separated and non-interacting defects is given as [2, 4, 66]

$$E_b = E_{\text{vacancy}}^F + E_{\text{substitution}}^F - E_{\text{vacancy-complex}}^F, \quad (3)$$

where E_{vacancy}^F , $E_{\text{substitution}}^F$ and $E_{\text{vacancy-complex}}^F$ are the formation energies of a single vacancy, a substitution and a vacancy-complex of $4H$ -SiC, respectively. Eq. 3 is interpreted as the energy released by the bonded vacancy-complex when formed from isolated vacancy and substitution. According to Eq. 3, in order to obtain a stable vacancy-complex, the binding energy of a particular vacancy-complex must be greater than zero. However if the vacancy-complex

binding energy is less than zero, then it is expected that the vacancy-complex will dissociate with an energy lower than the formation energy and hence it becomes unstable.

3. Results and Discussion

3.1. *P* related vacancy-complexes in 4H-SiC

For us to obtain the binding energy of the vacancy-complex, we calculated the formation energies of the non-interacting P_C , P_{Si} , V_C and V_{Si} . The calculated formation energies of the V_C and V_{Si} are 5.00 and 7.23 eV respectively. These results are in agreement with earlier reported results [22, 67, 68]. By using Eq. 1, we obtained the formation energy of the neutral charge state of the P_C and P_{Si} to be 6.78 and 1.29 eV, respectively. These results which are in agreement with earlier reported data [37, 69, 70] show that under equilibrium conditions, the P_{Si} and P_C are energetically stable. This suggests that P can be built in on both substitutional lattices, that is P_{Si} and P_C , with the former more energetically favourable. Since we are not interested in the defects levels induced in the band gap of 4H-SiC by non-interacting P_C and P_{Si} , we did not inject charge state into the system. Table 1 lists the energy of formation and the binding energies for the neutral charge state of the P related vacancy-complexes in 4H-SiC. Fig 2 displays a model of the relaxed geometric structures of 4H-SiC, and P-related vacancy-complexes ($P_{Si}V_C$ and P_CV_{Si}) presented in this report. Under equilibrium conditions, the binding energies of the $P_{Si}V_C$, P_CV_C , P_CV_{Si} and $P_{Si}V_{Si}$ in their rich chemical potential conditions for the neutral charge state are 2.00, 0.73, 3.40 and 0.01 eV, respectively. These positive binding energies suggest the possibility of the

respective vacancy-complexes to be stable and hence, dissociating into a well non-interacting defects will occur at the expense of higher formation energy. Whereas the formation energy of the $P_C V_C$ is 11.05 eV, for the $P_{Si} V_C$, a lower formation energy of 4.29 eV was obtained. For the $P_C V_{Si}$ the formation energy is 10.61 eV, while for the $P_{Si} V_{Si}$ a lower formation energy of 8.51 eV was obtained. The energy of formation of the $P_C V_{Si}$ for the neutral charge state under equilibrium conditions is relatively higher than that of the $P_{Si} V_{Si}$. One would have expected the binding energy of the $P_C V_{Si}$ to be lower than that of the $P_{Si} V_{Si}$, but this is not the case. This scenario can be attributed to the lower formation energy of the P_{Si} compare to that of the P_C . Furthermore, we observed that vacancy-complexes formed with the P_{Si} are more stable with lower formation energies compare to the others formed with the P_C . This observation is attributed to the fact that the energy of formation of the P_C is about 5.49 eV higher than that of the P_{Si} . In addition, the formation energy of the V_C for the neutral charge state under equilibrium conditions is lower than that of the V_{Si} . The $P_{Si} V_C$ is the most stable vacancy-complex compare to others. This is expected because the energies of formation for the P_{Si} and V_C are of the order of at least 3.00 eV lower than that of the P_C and V_{Si} . The low formation energy of the $P_{Si} V_C$ indicates its tendency to be observed in DLTS experimental technique as reported in Refs [69, 71].

To explore the defects levels induced in the band gap of the $4H$ -SiC by a vacancy-complex, we plotted the graph of the formation energy as a function of the Fermi energy as shown in Fig. 4. While the $P_{Si} V_C$ induced a shallow double donor level (+2/+1) at $E_V+0.37$ eV, the $P_C V_C$ induced double donor level is deeply lying at $E_V+0.93$ eV. Both the $P_{Si} V_C$ and $P_C V_C$ induced deep

single donor level (+/0) at $E_V+1.96$ and $E_V+2.29$ eV, respectively. The single and double donor levels induced by the $P_{Si}V_C$ and P_CV_C reveal that these defects are dominated by carbon vacancy. In addition, the $P_{Si}V_C$ donor level is below the donor level of the P_{Si} and above that of the V_C as reported in Ref [72]. Furthermore, a similar defect level observed for both the P_CV_C and $P_{Si}V_C$ is the single shallow acceptor (0/-1). This shallow acceptor level (0/-1) has an energy of $E_C-0.19$ eV for the P_CV_C , whereas for the $P_{Si}V_C$ the (0/-1) energy level is $E_C-0.20$ eV. The thermodynamic charge state transition levels induced by P_CV_{Si} are shallow for both the (+1/-1) and (-1/-2) levels. The (+1/-1) is a negative-U ordering which was caused by the large lattice distortion. A negative-U ordering was observed for the $P_{Si}V_{Si}$. While for the P_CV_{Si} , the (+1/-1) and (-1/-2) levels were $E_V+0.75$ and $E_C-0.16$ eV, respectively. For the $P_{Si}V_{Si}$, the (+1/-1) and (-1/-2) were $E_V+1.21$ and $E_C-0.03$ eV, respectively.

Based on the trend of the V_C and V_{Si} related complexes, we observed that the V_C related vacancy-complexes induced both double and single donor levels, whilst the V_{Si} related vacancy-complex induced a negative-U ordering. By using the method of Ref [51, 59], the effective-U (U^{eff}) of the negative-U ordering was calculated. While the P_CV_{Si} negative-U ordering is shallow with $U^{eff} = -0.15$ eV, for the $P_{Si}V_{Si}$ it is deep with $U^{eff} = -0.89$ eV. Whereas V_C related vacancy-complex induced a single acceptor level close to the conduction band edge, the V_{Si} related vacancy-complex induced a double acceptor level closed to the conduction band edge. The V_{Si} related vacancy-complex experienced large lattice distortion compared to the V_C related vacancy-complex and hence have a negative-U ordering. This implies

that these defects trapped two electrons (or holes) with the second bond more strongly than the first. The negative-U characteristic of these defects suggest that the energy gained by electron pairing is likely going to overcome the Coulombic repulsion of the two electrons at the site. This shows that the stability of the neutral charge state can never be observed since it is in the excited state.

For the $P_{Si}V_C$ and P_CV_C , the accommodation of P at a silicon or carbon site with a vacancy is dominated by the single positive charge state over half of the full theoretical band gap. For the P_CV_{Si} and $P_{Si}V_{Si}$ on the other hand, when P is at the carbon or silicon sites its accommodation is dominated by the single negative charge state which spanned almost 2/3 of the band gap of 4H-SiC. Except for the acceptor level, the defect levels induced by vacancy-complexes shown in Figs 4a and 4b are far away from the VBM, whereas the acceptor defect induced levels of the P_CV_{Si} and $P_{Si}V_{Si}$ are close to the CBM. Considering the fact that the results of the P_CV_{Si} and $P_{Si}V_C$ have been reported for the case of 3C-SiC [69], we therefore looked at the similarities between the same defects in 3C-SiC and 4H-SiC. The P_CV_{Si} and $P_{Si}V_C$ according to Refs [69, 72] induced deep donor level and shallow acceptor level in 3C-SiC, whereas in 4H-SiC the same defects induced deep donor and shallow acceptor levels in addition to the presence of negative-U charge state ordering. Furthermore, the researcher have shows that the stability of the P_CV_{Si} pair might not be possible in 3C-SiC, but for 4H-SiC, our results shows that the formation of P_CV_{Si} pairs is possible with a stable binding energy. Another interesting finding is that the $P_{Si}V_C$ is dominated by V_C for both the 3C-SiC and 4H-SiC.

3.2. Al related vacancy-complexes in 4H-SiC

In order to provide a theoretical insight into the activities of defects formed by Al substitution with either carbon or silicon vacancy, we explored these vacancy-complexes ($\text{Al}_{\text{Si}}\text{V}_{\text{C}}$, $\text{Al}_{\text{C}}\text{V}_{\text{C}}$, $\text{Al}_{\text{C}}\text{V}_{\text{Si}}$ and $\text{Al}_{\text{Si}}\text{V}_{\text{Si}}$). A model of relaxed geometric structures of the $\text{Al}_{\text{Si}}\text{V}_{\text{Si}}$ and $\text{Al}_{\text{C}}\text{V}_{\text{Si}}$ are shown in Fig. 3. Firstly, we calculated the formation energies of the neutral charge state of the Al_{C} and Al_{Si} . The formation energy of Al_{C} is about 11.00 eV higher than that of the Al_{Si} . These results suggest that the Al_{Si} is more stable and energetically favourable under equilibrium conditions than the Al_{C} . The V_{C} has been known to form with lower formation energy relative to the V_{Si} because it can diffuse under high temperature up to 1100 °C. The V_{C} is easily trapped by immobile Al_{Si} to form $\text{Al}_{\text{Si}}\text{V}_{\text{C}}$ vacancy-complex. Table 3 lists the energy of formation and the binding energies for the neutral charge state of the Al related vacancy-complex in 4H-SiC. Based on the result of the formation energy as listed in Table 3, the $\text{Al}_{\text{Si}}\text{V}_{\text{C}}$ is more energetically stable under equilibrium conditions with a formation energy of 3.73 eV for the neutral charge state. Furthermore, the formation energies of 16.91 and 17.41 eV, respectively for the $\text{Al}_{\text{C}}\text{V}_{\text{Si}}$ and $\text{Al}_{\text{C}}\text{V}_{\text{C}}$ are relatively higher than the 10.50 eV of the $\text{Al}_{\text{Si}}\text{V}_{\text{Si}}$ for the neutral charge state. This is attributed to the higher formation energy of the V_{Si} and Al_{C} compare to that of the V_{C} and Al_{Si} , respectively. As motivated earlier and also reported in literature, the energy of formation of the V_{Si} is always higher than the V_{C} , therefore we expect the difference in the formation energy to play a major role in the stability of these complexes with respect to their formation energies. In order to predict the stability of these defects with respect to their binding energies,

we calculated their binding energies using Eq. 3. In spite of the relatively high formation energy of the $\text{Al}_C\text{V}_{\text{Si}}$ compared to the $\text{Al}_{\text{Si}}\text{V}_{\text{Si}}$, it turns out that its binding energy of 4.83 eV is relatively higher than the binding energy 0.10 eV of the latter. So we can conclude that the $\text{Al}_{\text{Si}}\text{V}_{\text{Si}}$ is likely going to dissociate with lower formation energy than the $\text{Al}_C\text{V}_{\text{Si}}$. While the Al_CV_C is the least stable with respect to its formation energy, the Al_CV_C has a positive binding energy of 2.10 eV. This suggests that the Al_CV_C is stable and hence, dissociation can only occur at the expense of higher energy.

The defects levels induced by the $\text{Al}_{\text{Si}}\text{V}_C$, Al_CV_C , $\text{Al}_C\text{V}_{\text{Si}}$ and $\text{Al}_{\text{Si}}\text{V}_{\text{Si}}$ were explored. The plots of formation energy as a function of the Fermi level for Al-related vacancy-complexes in $4H$ -SiC are shown in Fig. 5. While the $\text{Al}_{\text{Si}}\text{V}_C$ and Al_CV_C acts as donor and induced a single donor level, the $\text{Al}_C\text{V}_{\text{Si}}$ and $\text{Al}_{\text{Si}}\text{V}_{\text{Si}}$ on the other hand, induced a double acceptor level in the band gap of $4H$ -SiC. For the Al_CV_C , the $(+1/0)$ and $(0/-1)$ defect levels are at energy of $E_V+1.73$ and $E_C-0.42$ eV, respectively. While the $(+1/0)$ is a deep level, the $(0/-1)$ is a shallow level lying close to the CBM. For the $\text{Al}_C\text{V}_{\text{Si}}$, the induced defect level $(-1/-2)$ is shallow with energy of $E_C-0.35$ eV. Additional interesting feature of the defect levels induced by the $\text{Al}_C\text{V}_{\text{Si}}$ is the $(+1/-1)$. This defect level is a negative-U ordering with an $U^{eff}=-0.05$ eV. This negative-U behaviour suggests the influence of large lattice distortion on the entire system and also shows that the ionized defect captured two electrons are well trapped with the second strongly bond. This resulted to the neutral charge state as a function of the Fermi energy always unstable and in an excited state. In this scenario, the possibility of the electrons to move from single positively to neutral charge state requires

a higher energy than for the same electron to move from single positively to single negatively charge state. Consequently, electron will move from charge state +1 to charge state -1 . Furthermore, the defect induced levels of $(+1/0)$ and $(0/-)$ for the $\text{Al}_{\text{Si}}\text{V}_{\text{C}}$ are deep levels with energy $E_{\text{V}}+1.60$ and $E_{\text{V}}+2.71$ eV, respectively. For the $\text{Al}_{\text{Si}}\text{V}_{\text{Si}}$ we observed the presence of a double acceptor level at $E_{\text{V}}+1.95$ eV. In addition, the $\text{Al}_{\text{Si}}\text{V}_{\text{Si}}$ shows that the single negatively charge state is more stable at the $\epsilon_{\text{F}}=0$, but as the ϵ_{F} is varied, deep almost at the middle of the band gap, the double negatively charge state becomes more accessible and stable even up to $\epsilon_{\text{F}}=E_{\text{C}}$.

4. Summary

We have used DFT from first-principles to predict the properties of various P and Al related vacancy-complexes in $4H$ -SiC: reporting their formation energies, binding energies, charge state transition levels and negative-U charge state ordering properties. The vacancy-complexes with silicon vacancy were predicted to experience more lattice distortion compared to those formed with carbon vacancy. The P and Al related vacancy-complexes showed that they are stable with respect to their binding energies under equilibrium conditions. While the vacancy-complexes formed by the P_{Si} and Al_{Si} are more energetically stable, the vacancy-complexes formed by P_{C} and Al_{C} had high formation energies. The $\text{P}_{\text{Si}}\text{V}_{\text{C}}$ and $\text{Al}_{\text{Si}}\text{V}_{\text{C}}$ are energetically most favourable defects at any Fermi-level in the band gap of $4H$ -SiC for P and Al related vacancy-complexes, respectively. This result also corroborate earlier report on the characterization of this defect. The defect levels induced by the P related vacancy-complexes are very shallow close to the conduction band

minimum for the single and double acceptor levels, and deep for both the single and double donor levels. Furthermore, only the $P_{Si}V_{Si}$ and P_CV_{Si} induced negative-U charge state ordering that are lying deep in the band gap of 4H-SiC. While the Al with V_C related vacancy-complexes on the other hand induced deep single donor and acceptor levels, the Al with V_{Si} induced only acceptor and negative-U charge state ordering. These results provide an insight for future work which is crucial for improving the quality of *n*-type SiC.

5. Acknowledgement

This work is supported partly by National Research foundation (NRF) of South Africa (Grant specific unique reference number (UID) 98961). The opinions, findings and conclusion expressed are those of the authors and the NRF accepts no liability whatsoever in this regard.

- [1] W. Li, L. Li, F. Wang, L. Zheng, J. Xia, F. Qin, X. Wang, Y. Li, R. Liu, D. Wang, et al., Chinese Physics B 26 (3) (2017) 037104.
- [2] E. Igumbor, R. E. Mapasha, R. Andrew, W. E. Meyer, Computational Condensed Matter 8 (2016) 31–35.
- [3] E. Igumbor, W. Meyer, Materials Science in Semiconductor Processing 43 (2016) 129–133.
- [4] E. Igumbor, R. E. Mapasha, W. E. Meyer, Journal of Electronic Materials 46 (7) (2017) 3880–3887.

- [5] I. D. Booker, H. Abdalla, J. Hassan, R. Karhu, L. Lilja, E. Janzén, E. Sveinbjörnsson, *Physical Review Applied* 6 (1) (2016) 014010.
- [6] W. Choyke, R. Devaty, L. Clemen, M. Yoganathan, G. Pensl, C. Hässler, *Applied physics letters* 65 (13) (1994) 1668–1670.
- [7] Q. Wahab, A. Ellison, A. Henry, E. Janzén, C. Hallin, J. Di Persio, R. Martinez, *Applied Physics Letters* 76 (19) (2000) 2725–2727.
- [8] R. Minamisawa, A. Mihaila, I. Farkas, V. Teodorescu, V. Afanas' ev, C.-W. Hsu, E. Janzén, M. Rahimo, *Applied Physics Letters* 108 (14) (2016) 143502.
- [9] H. Matsunami, T. Kimoto, *Materials Science and Engineering: R: Reports* 20 (3) (1997) 125–166.
- [10] V. Khranovskyy, I. Shtepliuk, L. Vines, R. Yakimova, *Journal of Luminescence* 181 (2017) 374–381.
- [11] E. Omotoso, W. Meyer, P. J. van Rensburg, E. Igumbor, S. Tunhuma, P. Ngoepe, H. Danga, F. Auret, *Nuclear Instruments and Methods in Physics Research Section B: Beam Interactions with Materials and Atoms* 409 (Supplement C) (2017) 241 – 245.
- [12] H. Danga, F. Auret, S. Tunhuma, E. Omotoso, E. Igumbor, W. Meyer, *Nuclear Instruments and Methods in Physics Research Section B: Beam Interactions with Materials and Atoms* 409 (Supplement C) (2017) 46 – 49.

- [13] C. Hemmingsson, N. Son, O. Kordina, E. Janzén, *Journal of applied physics* 91 (3) (2002) 1324–1330.
- [14] T. Kimoto, A. Itoh, H. Matsunami, S. Sridhara, L. Clemen, R. Devaty, W. Choyke, T. Dalibor, C. Peppermüller, G. Pensl, Nitrogen donors and deep levels in high-quality 4H–SiC epilayers grown by chemical vapor deposition, *Applied physics letters* 67 (19) (1995) 2833–2835.
- [15] S. Sridhara, L. Clemen, R. Devaty, W. Choyke, D. Larkin, H. Kong, T. Troffer, G. Pensl, Photoluminescence and transport studies of boron in 4H SiC, *Journal of applied physics* 83 (12) (1998) 7909–7919.
- [16] T. Troffer, M. Schadt, T. Frank, H. Itoh, G. Pensl, J. Heindl, H. Strunk, M. Maier, Doping of SiC by implantation of boron and aluminum, *physica status solidi (a)* 162 (1) (1997) 277–298.
- [17] T. Troffer, C. Peppermüller, G. Pensl, K. Rottner, A. Schöner, *Journal of applied physics* 80 (7) (1996) 3739–3743.
- [18] J. Weber, W. Koehl, J. Varley, A. Janotti, B. Buckley, C. Van de Walle, D. Awschalom, *Journal of Applied Physics* 109 (10) (2011) 102417.
- [19] X. Wang, M. Zhao, H. Bu, H. Zhang, X. He, A. Wang, *Journal of Applied Physics* 114 (19) (2013) 194305.
- [20] A. Gali, P. Deák, P. Ordejón, N. Son, E. Janzén, W. Choyke, *Physical Review B* 68 (12) (2003) 125201.
- [21] X. T. Trinh, K. Szász, T. Hornos, K. Kawahara, J. Suda, T. Kimoto, A. Gali, E. Janzén, N. T. Son, *Physical Review B* 88 (23) (2013) 235209.

- [22] K. Szász, V. Ivády, I. A. Abrikosov, E. Janzén, M. Bockstedte, A. Gali, *Physical Review B* 91 (12) (2015) 121201.
- [23] Z. Li, W. Zhou, X. Su, F. Luo, Y. Huang, C. Wang, *Journal of Alloys and Compounds* 509 (3) (2011) 973–976.
- [24] A. Csóré, H. von Bardeleben, J. Cantin, A. Gali, *Physical Review B* 96 (8) (2017) 085204.
- [25] T. Oda, Y. Zhang, W. J. Gr, Study of intrinsic defects in 3C-SiC using first-principles calculation with a hybrid functional, *The Journal of chemical physics* 139 (12) (2013) 124707.
- [26] E. Igumbor, O. Olaniyan, R. E. Mapasha, H. T. Danga, E. Omotoso, W. E. Meyer, *Journal of Physics: Condensed Matter* 30 (18) (2018) 185702.
- [27] H. Heissenstein, C. Peppermueller, R. Helbig, *Journal of applied physics* 83 (12) (1998) 7542–7546.
- [28] Y. Negoro, K. Katsumoto, T. Kimoto, H. Matsunami, *Journal of Applied Physics* 96 (1) (2004) 224–228.
- [29] F. Schmid, M. Laube, G. Pensl, G. Wagner, M. Maier, *Journal of applied physics* 91 (11) (2002) 9182–9186.
- [30] D. Okamoto, H. Yano, K. Hirata, T. Hatayama, T. Fuyuki, *IEEE Electron Device Letters* 31 (7) (2010) 710–712.
- [31] H. Yano, T. Kimoto, H. Matsunami, *Applied physics letters* 81 (2) (2002) 301–303.

- [32] D. Okamoto, H. Yano, T. Hatayama, T. Fuyuki, in: Materials Science Forum, vol. 645, Trans Tech Publ, 495–498, 2010.
- [33] V. Khemka, R. Patel, N. Ramungul, T. Chow, M. Ghezzi, J. Kretchmer, Journal of electronic materials 28 (3) (1999) 167–174.
- [34] M. Capano, R. Santhakumar, R. Venugopal, M. Melloch, J. Cooper, Journal of electronic materials 29 (2) (2000) 210–214.
- [35] M. A. Capano, J. Cooper Jr, M. Melloch, A. Saxler, W. Mitchel, Journal of Applied Physics 87 (12) (2000) 8773–8777.
- [36] T. Kimoto, K. Kawahara, B. Zippelius, E. Saito, J. Suda, Superlattices and Microstructures 99 (2016) 151 – 157.
- [37] M. Bockstedte, A. Mattheis, O. Pankratov, Applied physics letters 85 (1) (2004) 58–60.
- [38] M. Miyata, Y. Higashiguchi, Y. Hayafuji, Journal of Applied Physics 104 (12) (2008) 123702.
- [39] I. G. Ivanov, A. Henry, E. Janzén, Phys. Rev. B 71 (2005) 241201.
- [40] A. Gali, T. Hornos, N. Son, E. Janzén, W. Choyke, Physical Review B 75 (4) (2007) 045211.
- [41] T. Hornos, A. Gali, N. T. Son, E. Janzén, in: Materials science forum, vol. 556, Trans Tech Publ, 445–448, 2007.
- [42] J. Heyd, G. E. Scuseria, M. Ernzerhof, The Journal of Chemical Physics 118 (18) (2003) 8207–8215.

- [43] G. Kresse, J. Furthmüller, *Physical Review B* 54 (16) (1996) 11169.
- [44] G. Kresse, D. Joubert, *Physical Review B* 59 (3) (1999) 1758.
- [45] P. E. Blöchl, Projector augmented-wave method, *Physical Review B* 50 (24) (1994) 17953.
- [46] J. P. Perdew, K. Burke, M. Ernzerhof, *Phys. Rev. Lett.* 77 (1996) 3865–3868.
- [47] P. Deák, B. Aradi, T. Frauenheim, E. Janzén, A. Gali, *Phys. Rev. B* 81 (2010) 153203.
- [48] E. Igumbor, C. Ouma, G. Webb, W. Meyer, *Physica B: Condensed Matter* 480 (2016) 191–195.
- [49] H. Tahini, A. Chroneos, R. Grimes, U. Schwingenschlögl, H. Bracht, *Applied Physics Letters* 99 (7) (2011) 072112.
- [50] P. Śpiewak, J. Vanhellefont, K. Sueoka, K. Kurzydłowski, I. Romandic, *Materials Science in Semiconductor Processing* 11 (5) (2008) 328–331.
- [51] E. Igumbor, K. Obodo, W. E. Meyer, in: *Solid State Phenomena*, vol. 242, Trans Tech Publ, 440–446, 2015.
- [52] M. E. Levinshtein, S. L. Rumyantsev, M. S. Shur, John Wiley & Sons, 2001.
- [53] H. J. Monkhorst, J. D. Pack, *Phys. Rev. B* 13 (12) (1976) 5188–5192.
- [54] J. Sotys, J. Piechota, P. Strak, S. Krukowski, *Applied Surface Science* 393 (Supplement C) (2017) 168 – 179.

- [55] V. Ivády, J. Davidsson, N. T. Son, T. Ohshima, I. A. Abrikosov, A. Gali, *Physical Review B* 96 (16) (2017) 161114.
- [56] E. Janzén, A. Gali, P. Carlsson, A. Gällström, B. Magnusson, N. T. Son, *Physica B: Condensed Matter* 404 (22) (2009) 4354–4358.
- [57] Ö. Soykal, P. Dev, S. E. Economou, *Physical Review B* 93 (8) (2016) 081207.
- [58] S. B. Zhang, J. E. Northrup, *Phys. Rev. Lett.* 67 (1991) 2339–2342.
- [59] Freysoldt, Christoph, Grabowski, Blazej, Hickel, Tilmann, J. Neugebauer, Kresse, Georg, Janotti, Anderson, V. de Walle, C. G., *Rev. Mod. Phys.* 86 (2014) 253–305.
- [60] C. Freysoldt, J. Neugebauer, C. G. Van de Walle, *physica status solidi (b)* 248 (5) (2011) 1067–1076.
- [61] J.-I. Iwata, C. Shinei, A. Oshiyama, *Physical Review B* 93 (12) (2016) 125202.
- [62] D. Shrader, S. M. Khalil, T. Gerczak, T. R. Allen, A. J. Heim, I. Szlufarska, D. Morgan, *Journal of Nuclear Materials* 408 (3) (2011) 257–271.
- [63] L. Torpo, M. Marlo, T. Staab, R. Nieminen, *Journal of Physics: Condensed Matter* 13 (28) (2001) 6203.
- [64] B. Aradi, A. Gali, P. Deák, J. Lowther, N. Son, E. Janzén, W. Choyke, *Physical Review B* 63 (24) (2001) 245202.
- [65] M. Miyata, Y. Hayafuji, *Applied physics express* 1 (11) (2008) 111401.

- [66] G. Zollo, Y. J. Lee, R. M. Nieminen, *Journal of Physics: Condensed Matter* 16 (49) (2004) 8991.
- [67] L. Gordon, A. Janotti, C. G. Van de Walle, *Physical Review B* 92 (4) (2015) 045208.
- [68] J. Weber, W. Koehl, J. Varley, A. Janotti, B. Buckley, C. Van de Walle, D. D. Awschalom, Quantum computing with defects, *Proceedings of the National Academy of Sciences* 107 (19) (2010) 8513–8518.
- [69] E. Rauls, U. Gerstmann, T. Frauenheim, H. Overhof, *Physica B: Condensed Matter* 340 (2003) 184–189.
- [70] S. Greulich-Weber, *physica status solidi (a)* 162 (1) (1997) 95–151.
- [71] V. Vainer, V. Ilin, *Sov. Phys. Solid State* 23 (1981) 1432.
- [72] A. Gali, P. Deák, P. Briddon, R. Devaty, W. Choyke, *Physical Review B* 61 (19) (2000) 12602.

Table 1: The formation energy (E^F) and binding energy (E_B) in eV at $\varepsilon_F=0$ zero of P vacancy-complexes in $4H$ -SiC. All energies were calculated under defect rich-conditions.

	$P_C V_{Si}$	$P_C V_C$	$P_{Si} V_C$	$P_{Si} V_{Si}$
E^F	10.61	11.05	4.29	8.51
E_B	3.40	0.73	2.00	0.01

Table 2: The charge state transition ($\varepsilon(q/q')$) levels above the VBM in eV induced by P vacancy-complexes in 4H-SiC.

Vacancy-complex	(+2/ + 1)	(+1/0)	(0/ - 1)	(-1/ - 2)	(+1/ - 1)
$P_C V_C$	0.93	2.29	3.04	–	–
$P_C V_{Si}$	–	–	–	3.07	0.75
$P_{Si} V_C$	0.37	1.96	3.03	–	–
$P_{Si} V_{Si}$	–	–	–	3.20	1.21

Table 3: The formation energy (E^F) and binding energy (E_B) in eV at $\varepsilon_F = 0$ zero of Al vacancy-complexes in 4H-SiC. All energies were calculated under defect rich-conditions.

	$Al_C V_{Si}$	$Al_C V_C$	$Al_{Si} V_C$	$Al_{Si} V_{Si}$
E^F	16.91	17.41	3.73	10.50
E_B	4.83	2.10	4.55	0.10

Table 4: The charge state transition ($\varepsilon(q/q')$) levels above the VBM in eV induced by Al vacancy-complexes in 4H-SiC.

Vacancy-complex	(+1/0)	(0/ - 1)	(-1/ - 2)	(+1/ - 1)
$Al_C V_C$	1.73	2.81	–	–
$Al_C V_{Si}$	–	–	2.88	0.52
$Al_{Si} V_C$	1.60	2.71	–	–
$Al_{Si} V_{Si}$	–	–	1.95	–

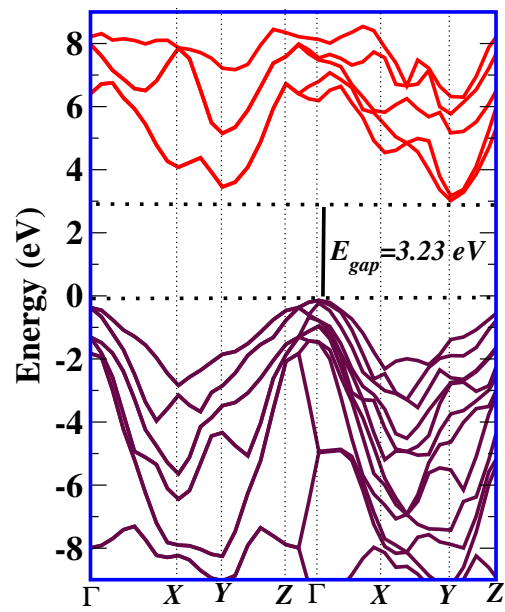


Figure 1: Band structure of 4H-SiC using the HSE06 hybrid functional. The band gap E_{gap} is 3.23 eV.

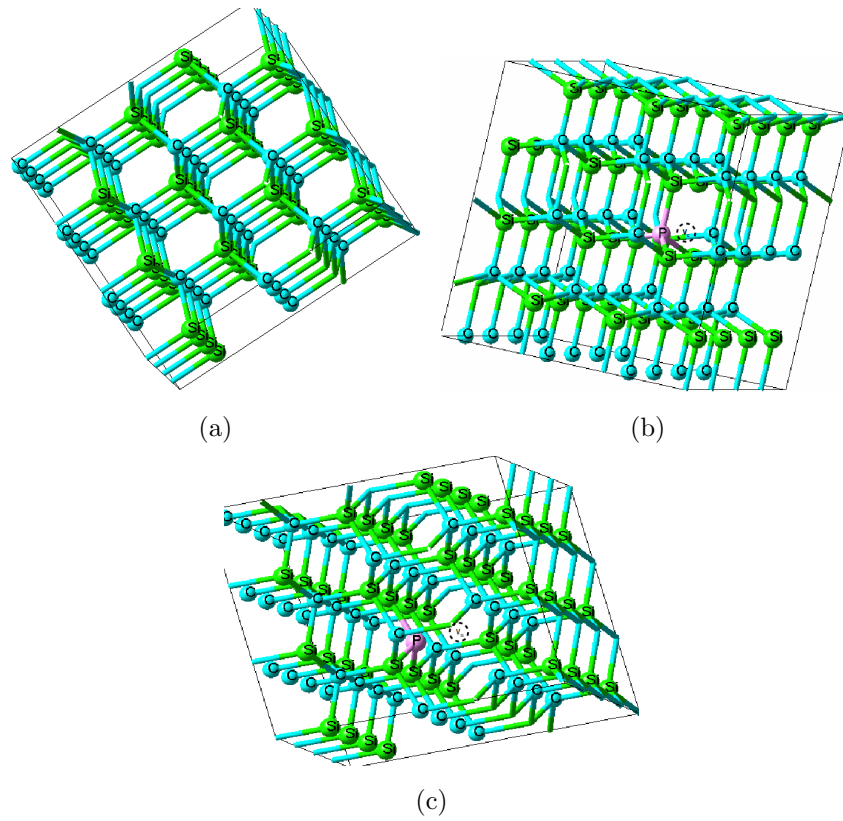


Figure 2: A model of the relaxed geometric structures of (a) $4H$ -SiC; (b) $P_{Si}V_C$ and (c) P_CV_{Si} .

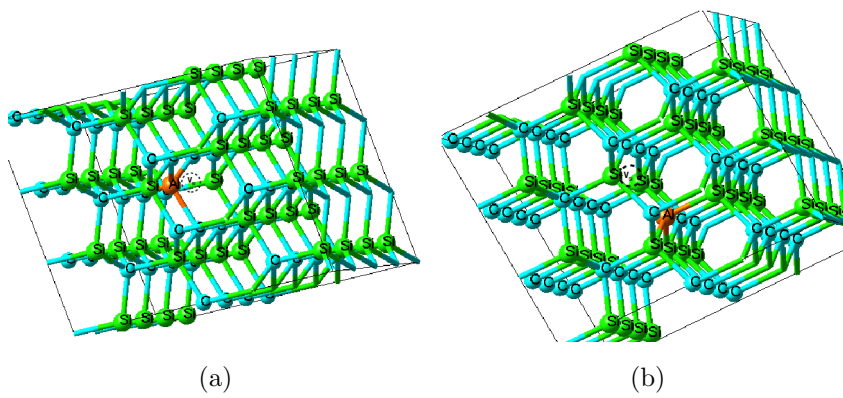


Figure 3: A model of the relaxed geometric structures of Al related vacancy-complexes in $4H$ -SiC (a) $Al_{Si}V_{Si}$ and (b) Al_CV_{Si} .

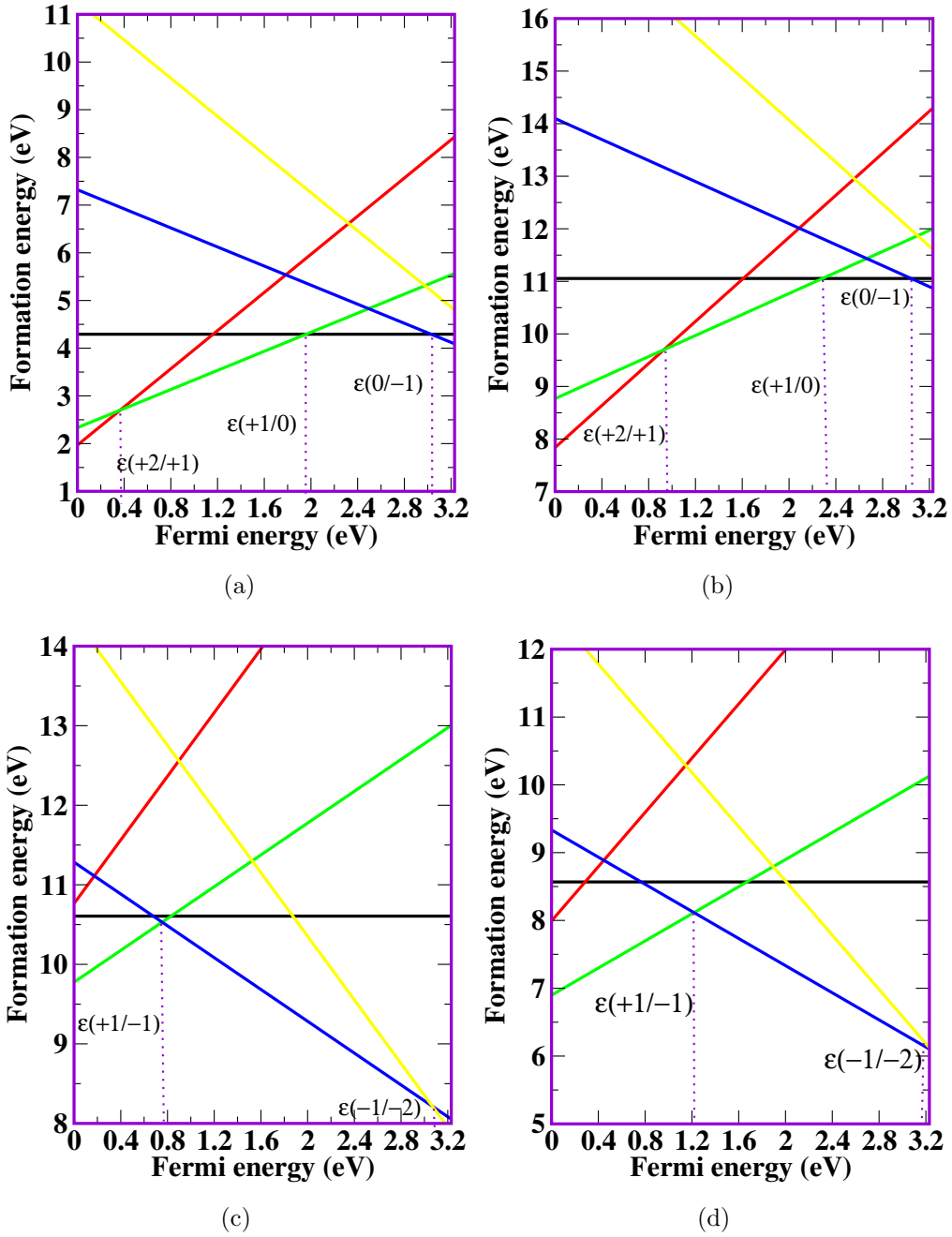


Figure 4: Plots of formation energy as a function of the Fermi energy in 4H-Si for the (a) $P_{Si}V_C$, (b) P_CV_C (c) P_CV_{Si} and (d) $P_{Si}V_{Si}$. The slope of each graph corresponds to the charge state as defined in Eq. 2.

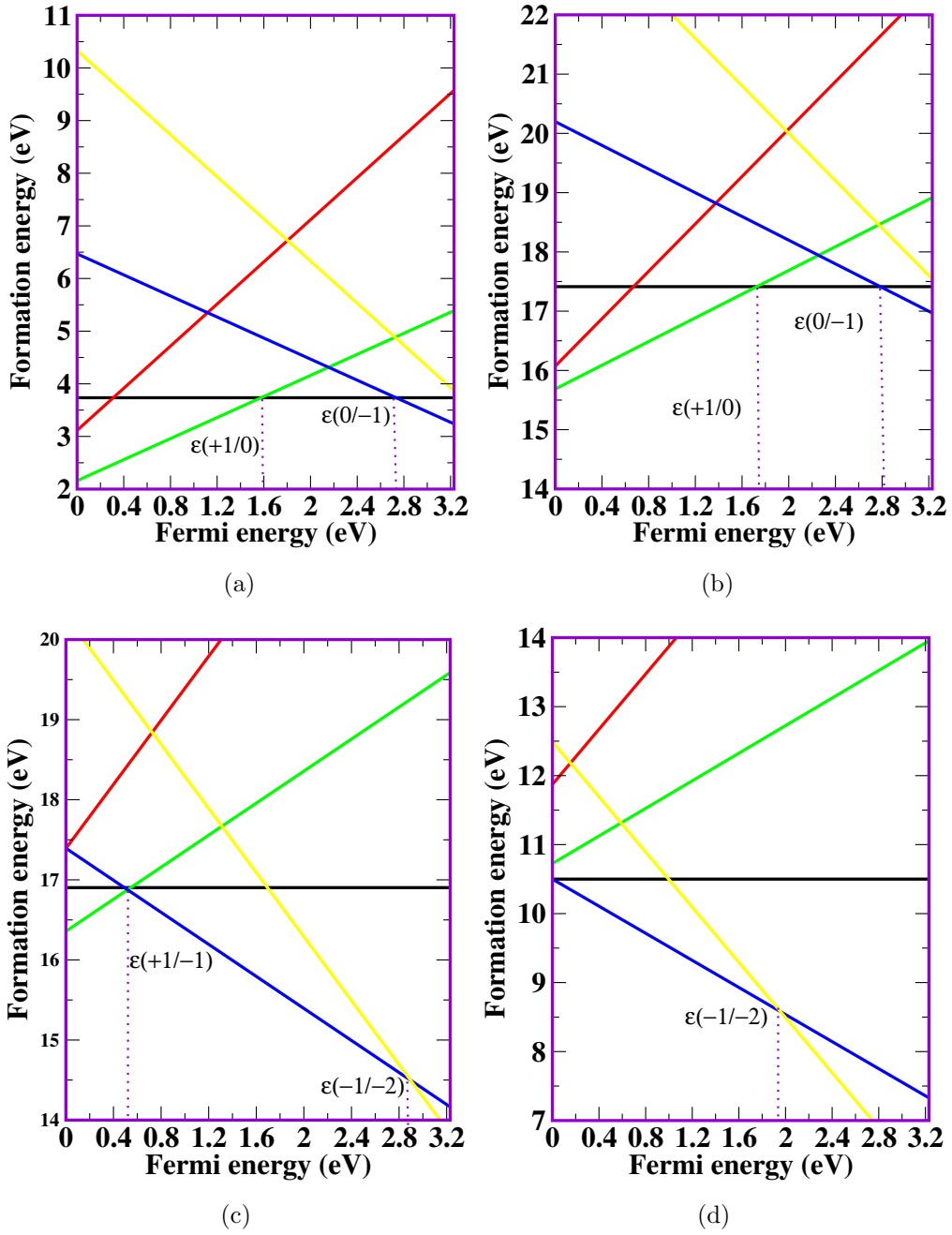


Figure 5: Plots of formation energy as a function of the Fermi energy in $4H$ -Si for the (a) $\text{Al}_{\text{Si}}\text{V}_C$, (b) Al_CV_C (c) $\text{Al}_C\text{V}_{\text{Si}}$ and (d) $\text{Al}_{\text{Si}}\text{V}_{\text{Si}}$. The slope of each graph corresponds to the charge state as defined in Eq. 2.